

Article

CO₂ Activation and Hydrogenation on Cu-ZnO/Al₂O₃ Nanorod Catalysts: An In Situ FTIR Study

Letian Wang^{1,2}, Ubong Jerome Etim¹, Chenchen Zhang¹, Lilac Amirav^{2,*}  and Ziyi Zhong^{1,3,*} 

¹ Department of Chemical Engineering, Guangdong Technion-Israel Institute of Technology (GTIIT), Shantou 515063, China; wang.letian@gtiit.edu.cn (L.W.); ubong.etim@gtiit.edu.cn (U.J.E.); chenchen.zhang@gtiit.edu.cn (C.Z.)

² Schulich Faculty of Chemistry, Technion-Israel Institute of Technology (IIT), Haifa 32000, Israel

³ Guangdong Provincial Key Laboratory of Materials and Technologies for Energy Conversion (MATEC), Guangdong Technion-Israel Institute of Technology (GTIIT), Shantou 515063, China

* Correspondence: lilac@technion.ac.il (L.A.); ziyi.zhong@gtiit.edu.cn (Z.Z.)

Abstract: CuZnO/Al₂O₃ is the industrial catalyst used for methanol synthesis from syngas (CO + H₂) and is also promising for the hydrogenation of CO₂ to methanol. In this work, we synthesized Al₂O₃ nanorods (n-Al₂O₃) and impregnated them with the CuZnO component. The catalysts were evaluated for the hydrogenation of CO₂ to methanol in a fixed-bed reactor. The support and the catalysts were characterized, including via in situ diffuse reflectance infrared Fourier transform spectroscopy (DRIFTS). The study of the CO₂ adsorption, activation, and hydrogenation using in situ DRIFT spectroscopy revealed the different roles of the catalyst components. CO₂ mainly adsorbed on the n-Al₂O₃ support, forming carbonate species. Cu was found to facilitate H₂ dissociation and further reacted with the adsorbed carbonates on the n-Al₂O₃ support, transforming them to formate or additional intermediates. Like the n-Al₂O₃ support, the ZnO component contributed to improving the CO₂ adsorption, facilitating the formation of more carbonate species on the catalyst surface and enhancing the efficiency of the CO₂ activation and hydrogenation into methanol. The synergistic interaction between Cu and ZnO was found to be essential to increase the space-time yield (STY) of methanol but not to improve the selectivity. The 3% CuZnO/n-Al₂O₃ displayed improved catalytic performance compared to 3% Cu/n-Al₂O₃, reaching a CO₂ conversion rate of 19.8% and methanol STY rate of 1.31 mmol_{cat}⁻¹h⁻¹ at 300 °C. This study provides fundamental and new insights into the distinctive roles of the different components of commercial methanol synthesis catalysts.

Keywords: CO₂ adsorption; CO₂ activation; CO₂ hydrogenation; CuZnO/Al₂O₃; catalyst components



Citation: Wang, L.; Etim, U.J.; Zhang, C.; Amirav, L.; Zhong, Z. CO₂ Activation and Hydrogenation on Cu-ZnO/Al₂O₃ Nanorod Catalysts: An In Situ FTIR Study. *Nanomaterials* **2022**, *12*, 2527. <https://doi.org/10.3390/nano12152527>

Academic Editor: Goran Drazic

Received: 30 June 2022

Accepted: 15 July 2022

Published: 23 July 2022

Publisher's Note: MDPI stays neutral with regard to jurisdictional claims in published maps and institutional affiliations.



Copyright: © 2022 by the authors. Licensee MDPI, Basel, Switzerland. This article is an open access article distributed under the terms and conditions of the Creative Commons Attribution (CC BY) license (<https://creativecommons.org/licenses/by/4.0/>).

1. Introduction

In the last two decades, global warming and related extreme weather conditions have become topical issues, and the mitigation of carbon dioxide (CO₂) release into the atmosphere is a top global priority. CO₂ is a major anthropogenic greenhouse gas (GHG) released during fossil fuel exploitation; thus, controlling CO₂ emissions is critical to maintaining the carbon-neutral state of the atmosphere [1–3]. The catalytic reduction of CO₂ with renewable hydrogen (H₂) to value-added chemicals and fuels such as hydrocarbons and alcohols represents a potential strategy to mitigate CO₂ emissions into the atmosphere [1,4–6]. For example, the hydrogenation of CO₂ to methanol is an important reaction in CO₂ conversion, as methanol can be used as a feedstock chemical and fuel [7]. However, CO₂ is a thermodynamically inert molecule that needs high reaction temperatures to activate the C=O bond. At high temperatures, the undesired reverse water-gas shift (RWGS) reaction is thermodynamically favored, which reduces the product selectivity. Therefore, developing a catalyst that can efficiently drive the process under mild conditions is imperative.

Different types of catalysts have been investigated for the thermocatalytic hydrogenation of CO₂ to methanol, including supported metal [8,9] and metal oxide [10,11]

catalysts. Cu-based catalysts have been reported to have the best activity for methanol production under industrially relevant conditions (5–10 MPa and 200–300 °C) [12,13]. The Cu-ZnO-Al₂O₃ catalyst prepared via the co-precipitation method is the industrial catalyst used for methanol production from CO + H₂; thus, the Cu-ZnO-based catalysts are widely investigated for CO₂ hydrogenation to methanol as well [14,15]. Various supports and promoters are explored for these catalysts, and different catalyst structures and active sites are reported [15–17]. The common supports or promoters for Cu-based catalysts include ZnO, ZnO-Al₂O₃, ZrO₂, TiO₂, In₂O₃, CeO₂, and SiO₂ [18,19]. At times the contribution of the support is complex. For example, Nitta et al. [18] observed significantly improved selectivity towards methanol formation at a low temperature upon introducing ZnO into Cu/ZrO₂. However, at high temperatures, adding ZnO promoted the methanol decomposition into CO, leading to a reduced yield for methanol.

Factors impacting the overall catalytic performance of the Cu-based catalysts include the nature of the support material, the Cu loading, the dispersion, and the preparation method [12,20]. However, their effects on the activation of CO₂ are still not clear. The specific roles of the different components within the industrial Cu-ZnO-Al₂O₃ catalyst for methanol synthesis from CO₂ were assigned in the literature [12,18]. ZnO is generally believed to be a multitasked component, acting as a physical spacer for the Cu particles and facilitating H₂ dissociation; Al₂O₃ plays the role of a structural promoter that increases Cu dispersion, whereas Cu drives the selectivity towards methanol [21,22]. However, further investigation is required to ascertain the individual roles of the catalyst components concerning CO₂ activation, as well as to better understand the observed synergetic effects within the complete system. In addition to the composition, the nature of the catalyst support and characteristics such as the morphology (size and shape), were also found to influence the CO₂ conversion efficiency and selectivity towards methanol formation [23–26]. An et al. [27] found that the catalytic activities of Cu/Zn/Al/Zr catalysts depended strongly on the morphology of the support, and the utilization of a fibrous shape improved the hydrogenation performance significantly. In addition, the proper selection of the catalyst support may provide additional advantages, such as reducing the amount of required active metal, inhibiting the sintering of the active metal, and prolonging the stability [22].

Diffuse reflectance infrared Fourier transform spectroscopy (DRIFTS) is a powerful technique for analyzing in situ substrate or adsorbate interactions, and has been previously utilized to characterize systems where the interactions of gases over the surface of a catalyst elucidated the catalytic surface chemistry [28–31].

In this work, we explored porous Al₂O₃ nanorods as the catalyst support in the CuZnO/Al₂O₃ catalysts for CO₂ hydrogenation. The Al₂O₃ nanorods were synthesized via the steam-assisted solid wet-gel method and deployed as a support for CuZnO. The CuZnO/Al₂O₃ catalyst was prepared using the incipient wetness impregnation method and evaluated for the hydrogenation of CO₂ to methanol. The catalysts supported on alumina nanorods exhibited better CO₂ reduction to methanol under the examined conditions than that supported on commercial alumina. Through a DRIFTS study, we gained a new understanding of the specific roles of Al₂O₃, ZnO, and Cu in CO₂ adsorption, activation, and hydrogenation reaction. This information will contribute to the design of catalysts with improved performance for industrial applications.

2. Experimental Section

2.1. Sample Preparation

(i) Nanorods Al₂O₃ preparation.

Al₂O₃ nanorods were synthesized using the steam-assisted solid wet-gel method according to the literature [32]. Typically, 30 g Al(NO₃)₃·9H₂O (>99.9%, SCR, Sinopharm Chemical Reagent Co., Ltd., Shanghai, China) was dissolved in 50 mL of deionized water. Approximately 15% NH₄OH aqueous solution (36%, SCR, Sinopharm Chemical Reagent Co., Ltd., Shanghai, China) was added dropwise to the aluminum nitrate solution at room temperature under stirring to control the pH at 5.0. The resulting solid precipitate was

recovered by filtration. The as-prepared solid cake-like wet gel was transferred to a glass beaker (25 mL) sitting in a Teflon vessel (200 mL), where 2 g of water was poured into the bottom of the vessel but was physically separated from the solid gel sample. The Teflon vessel was sealed and heated at 200 °C for 48 h. The obtained white solid material was washed with deionized water and recovered by centrifugation, dried at 60 °C for 24 h, and subsequently calcined in air at 600 °C for 5 h to obtain Al₂O₃ nanorods.

(ii) Catalyst preparation.

The Al₂O₃-supported CuZnO catalysts were prepared via the incipient wetness impregnation method using Cu(NO₃)₂·6H₂O and Zn(NO₃)₂·6H₂O (>99.9%, SCR, Sinopharm Chemical Reagent Co., Ltd., Shanghai, China) (mass ratio of Cu: ZnO = 2:1) as the Cu and Zn precursors. The catalysts are labeled here as CuZnO/n-Al₂O₃ and CuZnO/c-Al₂O₃, where n-Al₂O₃ and c-Al₂O₃ are Al₂O₃ nanorods and commercial Al₂O₃ (γ-Al₂O₃, >99.9%, Shanghai Macklin Biochemical Co., Ltd., Shanghai, China), respectively. The loading of the active component is referred to as the total weight loading of Cu and ZnO (Cu+ZnO) in the catalysts. The resulting samples were dried overnight at 60 °C and subsequently calcined in air at 400 °C for 4 h. Catalysts with Cu+ZnO loading of 3–20% and 3% Cu were studied.

2.2. Characterization

The crystallinity of the samples was characterized via X-ray diffraction (XRD) experiments performed on a Bruker D8 Advance X-ray diffractometer (Cu Kα) (Bruker Corporation Inc., Billerica, MA, USA). The diffraction patterns were acquired at a scanning step of 0.01° and a scanning speed of 10°/min. Transmission electron microscopy (TEM) and scanning electron microscopy (SEM) images of the samples were recorded on a Talos F200X transmission electron microscope (Thermo Fisher Scientific Inc., Waltham, MA, USA) operated at 300 kV and a scanning electron microscope (GeminiSEM 450, Carl ZEISS, Oberkochen, Germany), respectively.

In situ DRIFTS measurements were performed on a Nicolet iS50 FTIR instrument (Thermo Fisher Scientific Inc., Waltham, MA, USA). The scans were recorded from 4000 to 600 cm⁻¹. Here, 50 mg catalyst powder was placed in a high-pressure (0–10 MPa) DRIFT cell (HVC-DRP-5, Harrick Scientific Products Inc., NY, USA) equipped with ZnSe windows and reduced at 300 °C in a pure H₂ stream (30 mL/min) for 2 h, after which the sample was flushed with N₂ (40 mL/min) for 1 h and cooled to room temperature. The background subtractions were executed over different samples for testing in 40 mL/min N₂ under 2 MPa. Then, the reactant gas mixture (H₂ + CO₂, 3:1 ratio) at a flow rate of 40 mL/min was introduced into the sample cell and the spectra were collected at different temperatures, increasing by 3 °C/min at an interval of 19 s. For the CO₂ activation study, the sample cell was cooled to 250 °C. The background subtractions were similarly performed under 2 MPa. The CO₂ was switched into the reaction chamber and the spectra were recorded for up to 120 min, after which the inlet gas was changed to H₂ and the process lasted for another 1 h 40 min.

2.3. Catalytic Performance Evaluation

The CO₂ hydrogenation to methanol was performed in a high-pressure fixed-bed flow reactor. Here, 0.1 g catalyst was fixed in a quartz tube using quartz wool and then packed into a stainless steel tubular reactor. Prior to the catalytic measurements, the catalyst was reduced in a gas stream (10% H₂/N₂) at 300 °C for 2 h with a flow rate of 10 mL/min under atmospheric pressure. Then, the temperature was decreased to 200 °C and the reducing gas was replaced by reaction gas (CO₂ + H₂, 1:3 ratio). The reaction was X(CO₂) gas hourly space velocity (GHSV) of 7800 mL g⁻¹ h⁻¹. The products flowing out from the reactor passed through a tube connected to a temperature control box to maintain the temperature at 120 °C and were then analyzed using an online gas chromatographer (Shimadzu GC-2014C) equipped with a TCD and an FID. The data obtained from the GC

measurements were used to calculate the CO₂ conversion ($X(\text{CO}_2)$), CH₃OH selectivity (S_i), and methanol space–time yield ($STY_{\text{CH}_3\text{OH}}$) using Equations (1)–(3).

$$X(\text{CO}_2) = \frac{n_{\text{CO}_2, \text{in}} - n_{\text{CO}_2, \text{out}}}{n_{\text{CO}_2, \text{in}}} \times 100\% \quad (1)$$

$$S_i = \frac{n_{\text{products}, i}}{n_{\text{CO}_2, \text{in}} - n_{\text{CO}_2, \text{out}}} \times 100\% \quad (2)$$

$$STY_{\text{CH}_3\text{OH}} = \frac{\text{GHSV} \times 0.25}{22.4} \times \frac{X(\text{CO}_2)S_i}{10000} \quad (3)$$

3. Results and Discussion

3.1. Catalyst Structure, Morphology and Textural Properties

The XRD patterns of the n-Al₂O₃ support with various levels of CuZnO loadings are presented in Figure 1. The pattern of the catalyst support shows diffractions at the 2θ values of around 37.3, 39.4, 46.0, and 67.0°, characteristic of the γ-Al₂O₃ (JCPDS 04-0858). The patterns of calcined catalyst samples at low loadings (3% and 6% CuZnO) are quite similar to that of the n-Al₂O₃ support. No XRD peaks of CuO or ZnO can be observed, suggesting the high dispersion of CuO and ZnO, or possibly because the amount yielded in the XRD signal was close to the detection limit. In contrast to the observations for low loadings, prominent CuO XRD peaks can be observed for 10% and 20% CuZnO loadings at 35.7°, 38.6°, and 48.7° (JCPDS 80-1268).

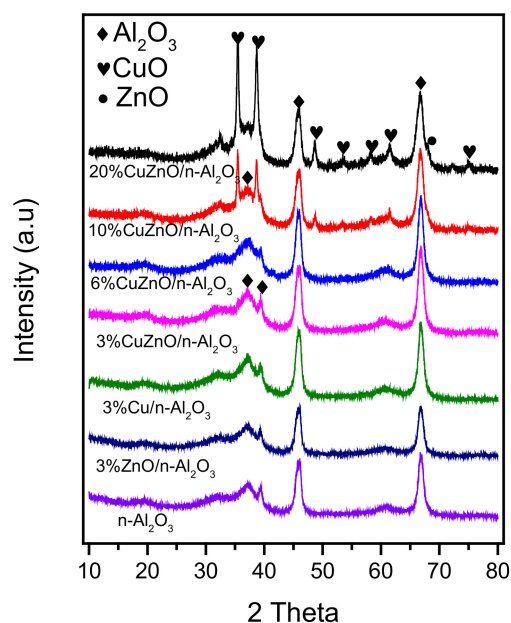


Figure 1. XRD patterns of n-Al₂O₃ and catalyst samples.

Figure 2a shows the morphology of the n-Al₂O₃ support, which can be described as γ-Al₂O₃ nanorods with lengths and widths of around 250–300 nm and 15–25 nm, respectively, in comparison with the spherical nano-sized particles of c-Al₂O₃ (figure not shown). The observed morphology is similar to that of the alumina nanorods reported in the literature [32,33]. Figure 2b shows the morphology of the n-Al₂O₃ impregnated with 3% CuZnO, and the corresponding EDX result presented in Table 1 shows a Cu/ZnO ratio of 2.25, which is reasonably close to the theoretical value of 2. The TEM micrographs of the n-Al₂O₃ and 3% CuZnO/n-Al₂O₃ catalysts are shown in Figure 3. After impregnating the n-Al₂O₃ support with 3% CuZnO, the morphology and structure of n-Al₂O₃ remained unchanged. Both materials consist of nanorods with pores of about 3–10 nm in diameter. Due to their low loadings and low contrast, it is difficult to visualize the CuO and ZnO

particles on the surface or inside the pores of the alumina nanorods with traditional wide-field TEM [34]. In Figure 4a, the linear isotherms of Cu/n-Al₂O₃, CuZnO/n-Al₂O₃, ZnO/n-Al₂O₃, and CuZnO/c-Al₂O₃ with corresponding BET surface areas of 94.4, 89.4, 67.6, and 99.3 m²/g, respectively, are shown. Except for CuZnO/c-Al₂O₃, other samples exhibit type IV isotherms with H1-type hysteresis loops, suggesting a typical mesoporous structure related to the n-Al₂O₃ support [35]. CuZnO/c-Al₂O₃ exhibits a type II isotherm with H4-type hysteresis loops, indicating an otherwise smaller mesoporous structure. According to the PSD curves (Figure 4b), CuZnO/c-Al₂O₃ possesses pores exhibiting a broad range but with an average pore width of 68 Å. Despite the n-Al₂O₃-supported samples exhibiting a wider pore size distribution, more of the pores are concentrated in the low-diameter region up to 150 Å. Cu/n-Al₂O₃ and CuZnO/n-Al₂O₃ have a nearly similar total pore volume of approximately 0.5 cm³/g, which is greater than those of ZnO/n-Al₂O₃ and CuZnO/c-Al₂O₃, 0.35 and 0.21 cm³/g, respectively.

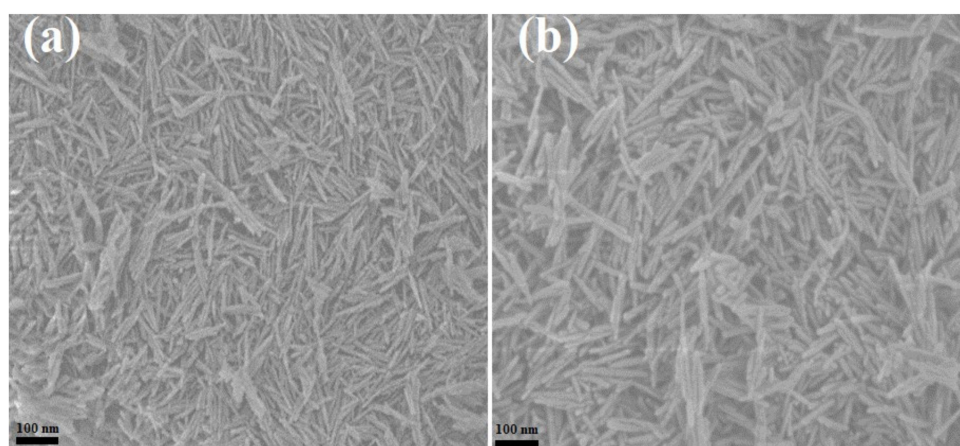


Figure 2. SEM images of (a) n-Al₂O₃ and (b) 3% CuZnO/n-Al₂O₃.

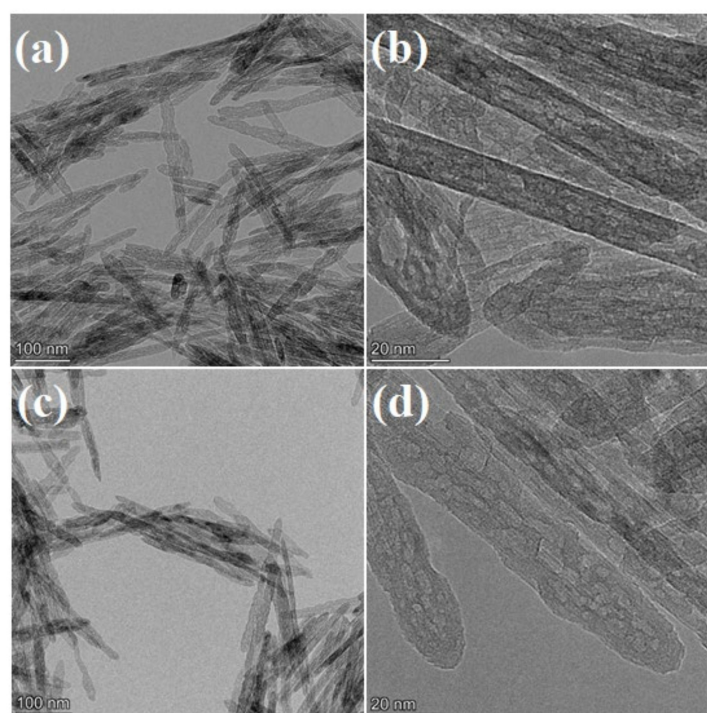
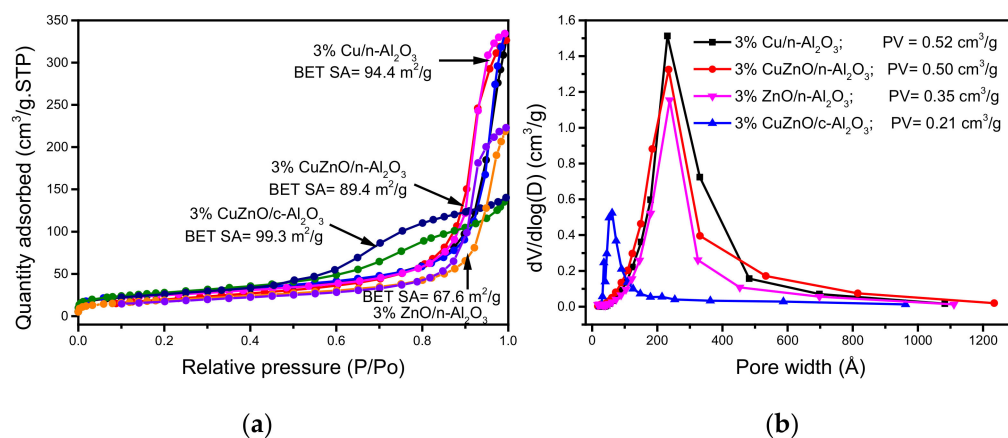


Figure 3. TEM images of (a,b) n-Al₂O₃ and (c,d) 3% CuZnO/n-Al₂O₃.

Table 1. EDX analysis of the 3% CuZnO/n-Al₂O₃ catalyst.

Element	Cu	Zn	Al	O
(At%)	0.81	0.29	40.57	58.33
(Wt%)	2.46	0.88	52.18	44.48

**Figure 4.** (a) Nitrogen adsorption–desorption isotherms and (b) pore size distribution curves of sample catalysts.

3.2. Catalytic Performance Evaluation

3.2.1. CO₂ Hydrogenation to Methanol

The catalytic performances, including the CO₂ conversion efficiency, selectivity towards methanol, and space–time yield for methanol formation, are presented in Figure 5. The influence of the temperature was examined in the range of 200 °C to 300 °C for the catalysts with CuZnO loadings from 3 to 20%, and the results are presented in Figure 5a. As expected, the CO₂ conversion increased with the temperature for all of the examined catalysts because the thermodynamically stable CO₂ molecule can be more efficiently broken down at high temperatures. However, at high reaction temperatures, the selectivity towards CH₃OH formation presented in Figure 5b decreased, given the competitive advantage of the RWGS reaction, resulting in CO formation [36]. The increasing CuZnO loading increased the CH₃OH selectivity from 58.5% for 3% CuZnO to 79.5% for 20% CuZnO at 200 °C, yet the improved selectivity did not essentially originate from increased CO₂ conversion efficiency. The catalysts with 6–20% CuZnO had relatively similar CO₂ conversion levels, higher than that of the catalyst containing 3% CuZnO by 12.6% at 300 °C. In addition, the methanol selectivity and STY of the former were higher than that of the latter at all temperatures (Figure 5b,c).

Since our aim was not to pursue a high efficiency for CO₂ conversion to methanol but rather to explore and understand the influence of the catalyst structure on its catalytic performance, as well as the fact that the catalyst with 3% CuZnO showed a more homogeneous distribution of CuZnO on the catalyst support than the catalyst with higher loadings, we focused on the catalytic performance of the 3% CuZnO catalyst. As shown in Figure 5d–f, different samples containing 3% Cu, 3% ZnO, or 3% CuZnO were compared to better ascertain the role of each component and the synergistic effect. In addition, the catalytic performance of 3% CuZnO/n-Al₂O₃ was compared with that of 3% CuZnO/c-Al₂O₃ (commercial Al₂O₃). As shown in Figure 5a–f, improved catalytic performance was observed, with better CO₂ conversion (19.8%) and STY_{CH₃OH} (1.31 mmol·g_{cat}^{−1}h^{−1}) at 300 °C while utilizing the 3% CuZnO/n-Al₂O₃ sample. This combination outperformed those of the separate components, as well as the sample supported on the commercial Al₂O₃. However, the methanol selectivity on 3% CuZnO/n-Al₂O₃ was lower than those of the Cu/n-Al₂O₃ and CuZnO/c-Al₂O₃ at temperatures above 220 °C (Figure 5e). The 3% ZnO/n-Al₂O₃ exhibited the lowest catalytic activity under all studied temperatures. This observation was

not unexpected because Cu is the main component that contributes to methanol selectivity. The pure n-Al₂O₃ support was found to have negligible activity for CH₃OH production (data not shown). Overall, CuZnO exhibited better reactivity than either Cu or ZnO. While Cu is the methanol-selective component, ZnO and Al₂O₃ play other roles in the catalytic process [12].

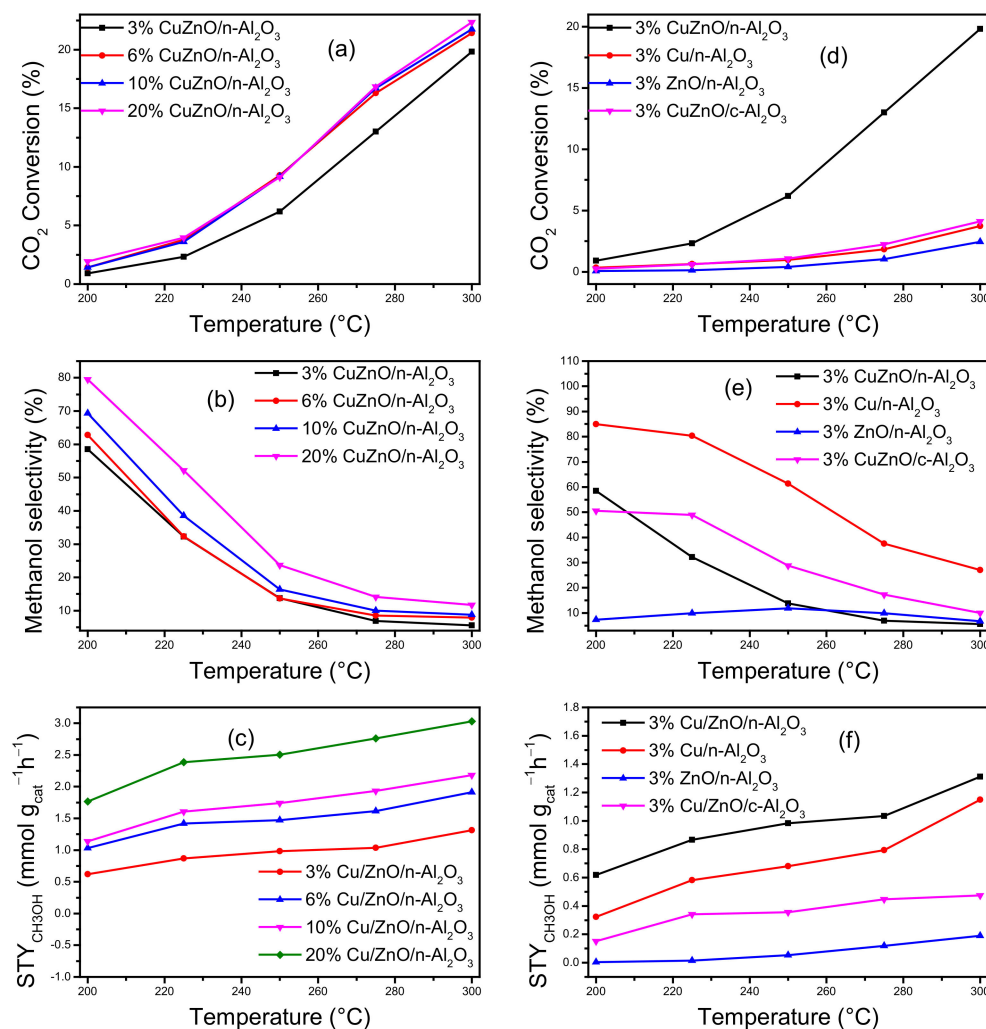


Figure 5. CO₂ hydrogenation performances of catalyst samples. (a) CO₂ conversion, (b) CH₃OH selectivity, and (c) STY_{CH₃OH} of CuZnO with various loadings, supported on n-Al₂O₃. (d) CO₂ conversion, (e) CH₃OH selectivity, and (f) STY_{CH₃OH} of 3% Cu, 3% ZnO, and 3% CuZnO on n-Al₂O₃, and 3% CuZnO on c-Al₂O₃. Reaction conditions: GHSV = 7800 mL g⁻¹ h⁻¹, gas flow rate = 13 mL min⁻¹, CO₂:H₂ = 1:3, P = 3.0 MPa.

3.2.2. DRIFTS Study on the CO₂ Activation

The CO₂ activation was investigated via in situ DRIFT spectroscopy [37,38]. First, CO₂ was adsorbed on the various fresh catalysts (at 250 °C, 2 MPa) that were reduced in H₂ at 300 °C and the spectra were recorded. After sufficient adsorption of CO₂ and attaining a stable state for up to 120 min, the inlet gas was changed to H₂. The spectra were again recorded for up to 220 min under the same conditions. The different catalyst components were studied during the experiments, and their specific roles in CO₂ activation and hydrogenation were elucidated.

(i) CO₂ activation on n-Al₂O₃

The pure n-Al₂O₃ in the CO₂ stream evolves bands at 1661, 1611, 1585, 1548, 1447, 1393, 1327, and 1228 cm⁻¹ attributed to carbonate species, indicating adsorption of CO₂ on Al₂O₃

(Figure 6a). Specifically, the bands at 1661, 1585, and 1447 cm^{-1} are those of bicarbonates (HCO_3^-) species [39]. Other bands at 1548 and 1327 cm^{-1} can be assigned to polydentate carbonate, while the band at 1393 cm^{-1} belongs to monodentate carbonate. The 1228 cm^{-1} band can be attributed to the $\delta(\text{OH})$ of bicarbonate species. This band decreases or even disappears with time. On the C-H stretching region in Figure 6b, bands can be observed at 3002, 2929, 2899–2896, 2875, 2769, and 2741 cm^{-1} . According to the literature, the bands at 3002 and 2769 cm^{-1} were assigned to bidentate formate species on Al_2O_3 -supported catalyst [40–42]; however, these bands were formed on pure alumina nanorods in this study. Here, we question the formation of formate species, since no H_2 gas was passed through the sample during the first 120 min, except that certain reactions exist with OH groups on the Al_2O_3 surface [37]. Upon passing H_2 gas through the sample, the band frequencies in the spectra did not change significantly, indicating that no substantial reaction occurred with the adsorbed carbon species and pointing to the fact that Al_2O_3 cannot or can poorly activate H_2 . In addition, the presence of H_2 may promote CO_2 desorption from the Al_2O_3 surface, since there was no strong reaction between them (CO_2 and Al_2O_3), as indicated by the disappearance of the band at 1228 cm^{-1} . This result indicates that nanorod Al_2O_3 can be used as a support for the CO_2 conversion catalyst due to its ability to adsorb CO_2 in its activated forms.

(ii) CO_2 activation on $\text{Cu}/\text{Al}_2\text{O}_3$ and $\text{ZnO}/\text{n-Al}_2\text{O}_3$

The formation of carbonate species on the surface of $\text{Cu}/\text{Al}_2\text{O}_3$ was obvious at 120 min, as evidenced by the bands at 1644, 1442, and 1228 cm^{-1} [39,42] (Figure 6c). Interestingly, these carbonate species disappeared and formate species formed after switching to H_2 . This indicates that Cu can activate H_2 and promote its reaction with adsorbed CO_2 species [43]. The formate species showed bands at 1662, 1585, 1395, and 1329 cm^{-1} . These bands were attributed to bidentate formate species on both Cu and Al_2O_3 and could be confirmed by the new bands at 2999, 2952, and 2742 cm^{-1} in the C-H stretching spectra (Figure 6d) [41,44]. Wang et al. [37] assigned the band at around 2999 cm^{-1} to the C-H bonds in unsaturated CH_x on CuNi catalysts, and its presence facilitated the deep hydrogenation of CO_2 to form methanol. For $\text{ZnO}/\text{n-Al}_2\text{O}_3$ (Figure 6e,f), after switching the feed gas from CO_2 to H_2 , there was no strong indication of H_2 activation; however, the appearance of bands of higher intensities and at nearly similar frequencies to that of pure $\text{n-Al}_2\text{O}_3$ is an indication that ZnO promoted the CO_2 adsorption on the catalyst surface. The prominence of bands at all frequencies, which originated when only CO_2 was adsorbed and maintained in the presence of H_2 , prove that ZnO activates CO_2 mainly as carbonates. However, some bands exhibited slight shifts in their positions, which indicates some sort of interaction and formation of formate species. In a previous study, the bands at 1385 and 1328 cm^{-1} were assigned to bidentate formate on ZnO and Al_2O_3 , whereas that at 1613 cm^{-1} was attributed to $V_{\text{as}}(\text{OCO})$ of a bidentate carbonate species on ZnO [45]. The formation of formate species on ZnO can be confirmed by the evolution of 2946 and 2841 cm^{-1} bands in the C-H stretch spectra.

(iii) CO_2 activation on $\text{CuZnO}/\text{Al}_2\text{O}_3$.

In the case of $\text{CuZnO}/\text{n-Al}_2\text{O}_3$, in the CO_2 gas stream, similar spectral features to $\text{Cu}/\text{n-Al}_2\text{O}_3$ were observed. The peaks at 1643 and 1434 cm^{-1} were those of $V_{\text{s}}(\text{OCO})$ of bicarbonate species [42]. The band at 1228 cm^{-1} was assigned to carboxylate ($\text{CO}_2^{\delta-}$) species in previous studies [38,46], but we related the band to the $\delta(\text{OH})$ of bicarbonate species, as earlier mentioned. However, the peak intensities were found to be higher than those obtained from $\text{Cu}/\text{n-Al}_2\text{O}_3$. This was attributed to the contribution of ZnO, which promotes CO_2 adsorption. After switching the gas to H_2 , most of the formed carbonate species converted into the formate species by reacting with H-atoms. This was evident from analyzing the bands at 1616, 1585, 1388, and 1326 cm^{-1} , which indicated formate species on Al_2O_3 , ZnO, and Cu [41,45]. The increased band intensities at 2897, 2921, and 2995 cm^{-1} indicated that the evolution of bidentate formate on the catalyst increased with time. It follows that $\text{CuZnO}/\text{n-Al}_2\text{O}_3$ exhibited the best CO_2 activation, good H_2 activation, and

catalytic activity for converting carbonate into formate, which is an important intermediate for methanol production. The increase in peak intensity means that the CO₂ adsorption intensified with time and reached a maximum (steady-state) at 120 min.

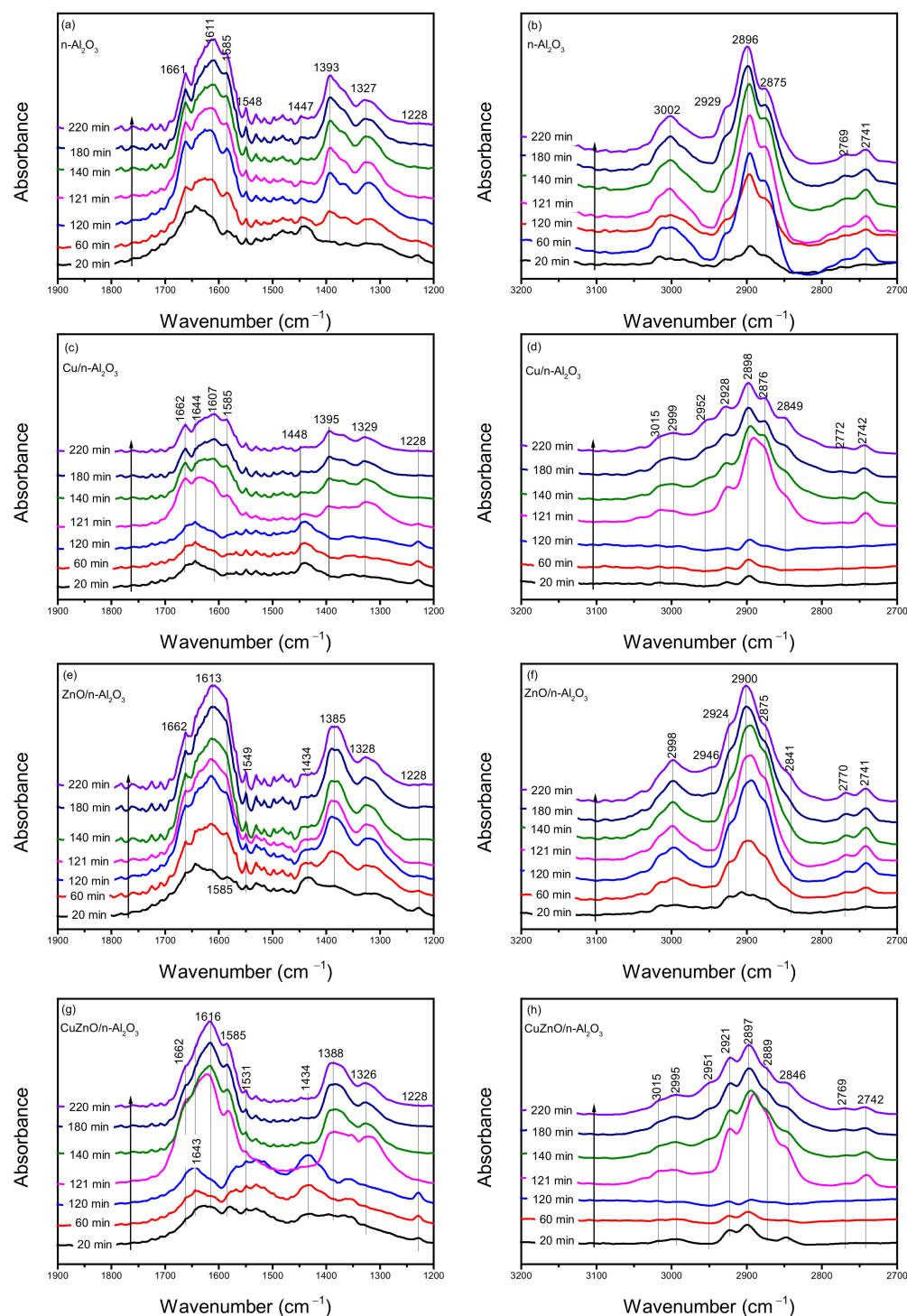


Figure 6. In situ DRIFT spectra at different times for the fresh catalysts (reduced in H₂ at 300 °C, purged in N₂, and then switched to CO₂ gas): (a,b) n-Al₂O₃, (c,d) 3% Cu/n-Al₂O₃, (e,f) 3% ZnO/n-Al₂O₃, and (g,h) 3% CuZnO/n-Al₂O₃ at 250 °C under 2 MPa for both pure CO₂ gas (0–120 min) and after switching the feed gas to H₂ (120–220 min).

3.2.3. DRIFTS Study of Methanol Formation from CO₂ Hydrogenation

The key surface species and intermediates involved in forming methanol over the catalysts are shown in Figure 7. The in situ DRIFT spectra collected at different temperatures on n-Al₂O₃, ZnO/Al₂O₃, Cu/n-Al₂O₃, and CuZnO/n-Al₂O₃ dosed with the reaction gas mixture indicated that the hydrogenation of CO₂ was initiated at a temperature above 50 °C. The initiation temperature decreases when the catalyst contains an active phase (Figure 7d,f,h). Except for the band around 1228 cm⁻¹, which is associated with δ(OH) of bicarbonate species or weakly adsorbed carbonate species (CO₃²⁻) that are desorbed at high temperatures, there is an increase in the intensities of the bands of hydrogenated species as the temperature rises. This means that the formation of key surface species increases with the temperature. The peaks at 1644 and 1416 cm⁻¹ are attributed to bicarbonate species formed when the reaction gas mixture passed through n-Al₂O₃ at 50 °C (Figure 7a). At higher temperatures, formate species formation is evident, typically indicated by the bands at 1612, 1583, 1391, and 1329 cm⁻¹. The formate species are also confirmed with the C-H stretching bands at 2997 and 2902 cm⁻¹ in Figure 7b, which are identical to those observed when formic acid is adsorbed and evacuated at 473 K on Al₂O₃ [41]. In Figure 7e,f, the bands at 1661, 1608, 1582, 1389, and 1325 cm⁻¹ are attributed to formate species on Cu and Al₂O₃ [40]. Specifically, the band at 1325 cm⁻¹ is for V_s(OCO) of bidentate formate species on Cu [40,41]. Other bands also evolved at 2931 and 2740 cm⁻¹, related to ν(C-H)+ν_{as}(OCO) and ν(C-H)+ν_s(OCO) of bidentate formate on Al₂O₃ [40]. On CuZnO/n-Al₂O₃ (Figure 7g,h), the reaction gas is adsorbed as carbonate species up to 100 °C, as indicated by the adsorption bands around 1526 and 1415 cm⁻¹ for polydentate carbonate and bicarbonate species, respectively [40]. The formation of formate species can be related to the bands at 1666 and 1628 cm⁻¹. The bidentate formate species on ZnO and Al₂O₃ showed bands of higher intensities at 1575, 1388, 1314, 2888, and 2740 cm⁻¹ [41,45]. Meanwhile, the 2921 cm⁻¹ band can be assigned to the ν(C-H) and δ(C-H)+ν_{as}(OCO) of bidentate formate on Cu [41,44]. The peaks at 2948 and 2843 in the CuZnO/n-Al₂O₃ spectra and at 2931 and 2846 in the Cu/n-Al₂O₃ spectra indicate the formation of methoxy species [30]. At 150 °C or higher temperatures, the band intensities increased compared with those of Cu/n-Al₂O₃. For these catalysts, the carbonate conversion to formate species is seen on both CuZnO and Cu, but the formation of formate species begins at a low temperature (100 °C) exclusively on Cu/n-Al₂O₃. The key intermediate species formed at different temperatures are summarized in Table 2. The introduction of ZnO enhances the CO₂ adsorption and facilitates more carbonate species formation. This, in turn, boosts the formate production through hydrogenation via dissociated H atoms, which spillover to the catalyst surface. The formation of formate at a lower temperature on the CuZnO/n-Al₂O₃ catalyst might be ascribed to a more effective H₂ dissociation in the presence of ZnO [40]. Generally, two reaction pathways for the hydrogenation of the CO₂ to methanol have been identified: RWGS + CO-hydro, along with formate pathways [47]. However, many studies on Cu-based catalysts conform to the formate pathway [30,38]. In this study, CO₂ is activated as carbonate species on the catalyst surface under the examined reaction conditions. As the temperature increases, H₂ is better activated and spills over to the catalyst surface, where it reacts with the carbonate and forms formate and methoxy species. Further hydrogenation of the surface species produces methanol. This mechanism is, thus, in good agreement with literature reports for other Cu-based systems.

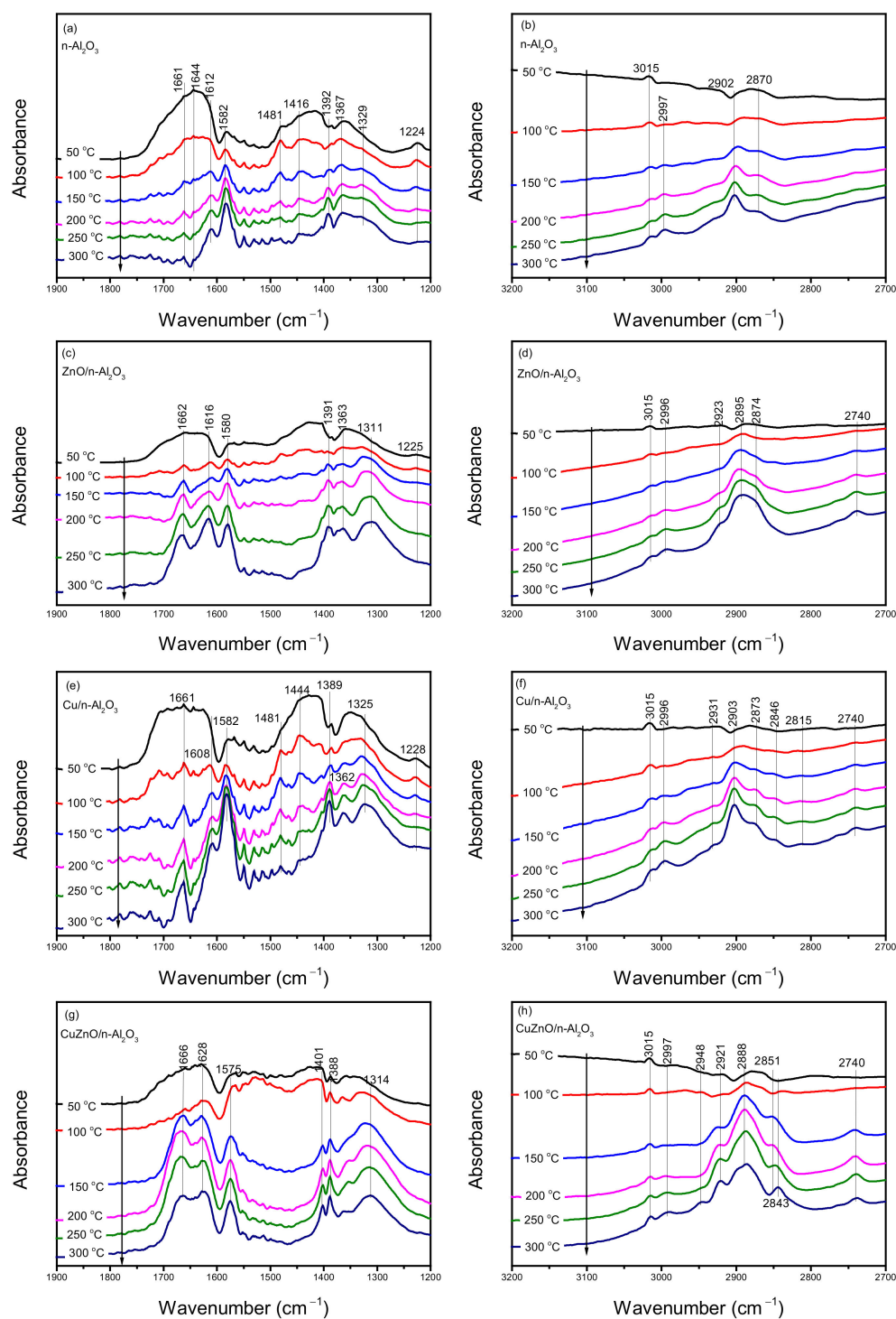


Figure 7. In situ DRIFT spectra of the reaction gas mixture of (a,b) $n\text{-Al}_2\text{O}_3$, (c,d) 3% $\text{ZnO}/n\text{-Al}_2\text{O}_3$, (e,f) 3% $\text{Cu}/n\text{-Al}_2\text{O}_3$, and (g,h) 3% $\text{CuZnO}/n\text{-Al}_2\text{O}_3$. Reaction conditions: $\text{CO}_2:\text{H}_2 = 1:3$, gas flow rate = 30 mL min^{-1} , $P = 2.0 \text{ MPa}$.

Table 2. Formation of the key intermediates and their peak intensity changes with temperature and catalyst composition *.

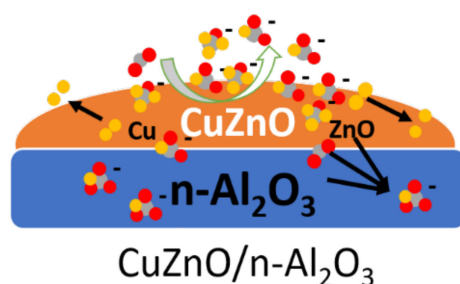
Temperature (°C)	n-Al ₂ O ₃	3% ZnO/n-Al ₂ O ₃	3% Cu/n-Al ₂ O ₃	3%CuZnO/n-Al ₂ O ₃
50	Bicarbonate	Bicarbonate (ZnO), bicarbonate (Al ₂ O ₃)	Bicarbonate (Al ₂ O ₃)	Bicarbonate (ZnO)
100	Bicarbonate ↓, monodentate, carbonate bidentate formate	Bidentate carbonate (ZnO) ↓, bicarbonate (Al ₂ O ₃) ↓, polydentate carbonate (Al ₂ O ₃ or ZnO), bidentate formate (ZnO and Al ₂ O ₃)	Bicarbonate (Al ₂ O ₃) ↓, bidentate formate (Al ₂ O ₃), polydentate carbonate	Bicarbonate (ZnO) ↓, polydentate carbonate (Al ₂ O ₃)
150	Bicarbonate ↓, polydentate carbonate, bidentate formate ↑	Bidentate formate (ZnO and Al ₂ O ₃) ↑, monodentate carbonate (Al ₂ O ₃) ↓, bicarbonate (Al ₂ O ₃) ↓, polydentate carbonate (Al ₂ O ₃) ↑	Bicarbonate (Al ₂ O ₃) ↓, bidentate formate (Cu), bidentate formate (Al ₂ O ₃) ↑	Bicarbonate (ZnO) ↑, polydentate carbonate (Al ₂ O ₃), bidentate formate (Al ₂ O ₃ and ZnO), bidentate formate (Cu), bidentate formate (ZnO) ↑, methoxy
200	Bicarbonate ↓, monodentate carbonate ↓, bidentate formate ↑	Bicarbonate (ZnO) ↑, bidentate carbonate (ZnO) ↑, bidentate formate (ZnO and Al ₂ O ₃) ↑, polydentate carbonate (ZnO) ↑	Bicarbonate (Al ₂ O ₃) ↓, bidentate formate (Cu), bidentate formate (Al ₂ O ₃) ↑, methoxy	Bidentate formate (Al ₂ O ₃ and ZnO) ↑, bidentate formate (Cu) ↑, bidentate formate (ZnO) ↑, bidentate formate (Al ₂ O ₃), methoxy
250	Bicarbonate ↓, nonodentate carbonate ↓, polydentate carbonate ↓, bidentate formate ↑	Bicarbonate (ZnO) ↑, bidentate carbonate (ZnO) ↑, bidentate formate (ZnO and Al ₂ O ₃) ↑, formate (Al ₂ O ₃) ↑	Bidentate formate (Cu) ↑, bidentate formate (Al ₂ O ₃) ↑, methoxy ↑	Bidentate formate (Al ₂ O ₃ and ZnO) ↑, bidentate formate (Cu) ↑, bidentate formate (ZnO) ↑, bidentate formate (Al ₂ O ₃) ↑, methoxy ↑
300	Same as in 250 °C	Bicarbonate (ZnO) ↑, bidentate carbonate (ZnO) ↑, bidentate formate (ZnO and Al ₂ O ₃) ↑, formate (Al ₂ O ₃) ↑	Same as in 250°C	Bidentate formate (Al ₂ O ₃ and ZnO) ↑, bidentate formate (Cu) ↑, Bidentate formate (ZnO) ↑, bidentate formate (Al ₂ O ₃) ↑, methoxy ↑

* ↓—Decrease; ↑—increase.

3.3. Roles of Al₂O₃, ZnO, and Cu in CO₂ Hydrogenation to Methanol

Understanding the structure–function relationship of a composite catalyst is important to develop more efficient catalysts for industrial applications. The individual roles of Al₂O₃, ZnO, and Cu and their synergistic effects in the CuZnO/Al₂O₃ catalyst used for the CO₂-to-methanol synthesis were investigated using DRIFT spectroscopy. Al₂O₃ is a large surface area support material with an appropriate surface for dispersing and stabilizing the active phase and slowing the sintering during the reaction at high temperatures [40]. Herein, we found Al₂O₃ to be a good material for CO₂ adsorption and activation to produce bicarbonate, carbonate, and formate species; the bicarbonate and carbonate species are converted into formate and methoxy in the presence of metal species that can activate H₂. The 3% Cu/n-Al₂O₃ and 3%CuZnO/n-Al₂O₃ catalysts possess nearly similar BET surface areas of 94.4 and 89.4 m²/g, respectively. This shows that both active phases had the same impact on the surface area; however, the catalysts exhibit slight differences in their CO₂ adsorption and catalytic activities. Methoxy and increasing amounts of formate species are produced for both catalysts. The conversion of carbonates to formate is evident, as H-atoms are available for the reaction after activation on Cu particles following the spillover effect. According to the catalytic performance and in situ DRIFT results, CuZnO/n-Al₂O₃ exhibited the best performance due to the synergistic effect resulting from the interaction of Cu and ZnO. Apparently, as ascertained from the in situ DRIFT spectra, the presence of ZnO with Cu promotes CO₂ adsorption and formate formation. The enhanced formate formation is thought to be due to additional H₂ dissociation activity. We, thus, suggest that ZnO also promotes H₂ activation. It was previously reported that a defective ZnO_x overlayer formed in a Cu/ZnO catalyst could dissociate H₂, even at room temperature [40]. From the above

discussion, it will be reasonable to conclude from our study that the different components of the industrial catalyst for methanol synthesis from CO₂ play different roles but with a cooperative effect in methanol formation, as shown in Scheme 1.



Scheme 1. Formation of key intermediate species in hydrogenation of CO₂ to methanol ( bicarbonate,  formate,  methoxy,  hydrogen).

4. Conclusions

Cu-based catalysts supported on Al₂O₃ nanorods for CO₂ activation and subsequent hydrogenation to methanol are discussed in this study. Compared with the commercial Al₂O₃ support, catalysts using Al₂O₃ nanorods as the support show higher efficiency for CO₂ conversion between 200 and 300 °C, but the methanol selectivity becomes lower above 220 °C. There is improved CO₂ adsorption on the Al₂O₃ nanorods. CO₂ is adsorbed and activated on the catalyst surface as carbonate species, which upon subsequent H₂ dissociation on Cu hydrogenates to formate species by reacting with the H atom. ZnO promotes CO₂ adsorption and probably facilitates H₂ dissociation on Cu, also leading to the more efficient hydrogenation of activated CO₂ species on CuZnO/Al₂O₃. This study will help to tailor the properties and composition of the Cu-based catalyst system to achieve higher efficiency for methanol synthesis from CO₂.

Author Contributions: Conceptualization, Z.Z.; Investigation, L.W. and C.Z.; Supervision, L.A. and Z.Z.; Writing—original draft, L.W.; Writing—editing and review, U.J.E., Z.Z. and L.A. All authors have read and agreed to the published version of the manuscript.

Funding: This research was funded by Guangdong Provincial Key Laboratory of Materials and Technologies for Energy Conversion (MATEC), by the GTIIT Project KD2000079, Guangdong Technion—Israel Institute of Technology, the 2020 Li Ka Shing Foundation Cross-Disciplinary Research Grant (2020LKSF09A), and the Guangdong Province Key discipline fund (GTIIT) in 2022.

Acknowledgments: The authors acknowledge the financial support by Guangdong Provincial Key Laboratory of Materials and Technologies for Energy Conversion (MATEC), GTIIT; the Li Ka Shing Foundation for Cross-Disciplinary Research, and the Guangdong Province.

Conflicts of Interest: The authors declare no conflict of interest.

References

1. Porosoff, M.D.; Yan, B.; Chen, J.G. Catalytic reduction of CO₂ by H₂ for synthesis of CO, methanol and hydrocarbons: Challenges and opportunities. *Energy Environ. Sci.* **2016**, *9*, 62–73. [[CrossRef](#)]
2. Wang, Q.; Luo, J.; Zhong, Z.; Borgna, A. CO₂ capture by solid adsorbents and their applications: Current status and new trends. *Energy Environ. Sci.* **2011**, *4*, 42–55. [[CrossRef](#)]
3. Wang, J.; Huang, L.; Yang, R.; Zhang, Z.; Wu, J.; Gao, Y.; Wang, Q.; O'Hare, D.; Zhong, Z. Recent advances in solid sorbents for CO₂ capture and new development trends. *Energy Environ. Sci.* **2014**, *7*, 3478–3518. [[CrossRef](#)]
4. Aresta, M.; Dibenedetto, A.; Angelini, A. Catalysis for the Valorization of Exhaust Carbon: From CO₂ to Chemicals, Materials, and Fuels. Technological Use of CO₂. *Chem. Rev.* **2014**, *114*, 1709–1742. [[CrossRef](#)]
5. Porosoff, M.D.; Yang, X.; Boscoboinik, J.A.; Chen, J.G. Molybdenum Carbide as Alternative Catalysts to Precious Metals for Highly Selective Reduction of CO₂ to CO. *Angew. Chem. Int. Ed.* **2014**, *53*, 6705–6709. [[CrossRef](#)]
6. Studt, F.; Sharafutdinov, I.; Abild-Pedersen, F.; Elkjær, C.F.; Hummelshøj, J.S.; Dahl, S.; Chorkendorff, I.; Nørskov, J.K. Discovery of a Ni-Ga catalyst for carbon dioxide reduction to methanol. *Nat. Chem.* **2014**, *6*, 320–324. [[CrossRef](#)]
7. Sehested, J. Industrial and scientific directions of methanol catalyst development. *J. Catal.* **2019**, *371*, 368–375. [[CrossRef](#)]

8. De, S.; Dokania, A.; Ramirez, A.; Gascon, J. Advances in the Design of Heterogeneous Catalysts and Thermocatalytic Processes for CO₂ Utilization. *ACS Catal.* **2020**, *10*, 14147–14185. [[CrossRef](#)]
9. Kattel, S.; Liu, P.; Chen, J.G. Tuning selectivity of CO₂ hydrogenation reactions at the metal/oxide interface. *J. Am. Chem. Soc.* **2017**, *139*, 9739–9754. [[CrossRef](#)]
10. Wang, J.; Zhang, G.; Zhu, J.; Zhang, X.; Ding, F.; Zhang, A.; Guo, X.; Song, C. CO₂ hydrogenation to methanol over In₂O₃-based catalysts: From mechanism to catalyst development. *ACS Catal.* **2021**, *11*, 1406–1423. [[CrossRef](#)]
11. Lin, L.; Wang, G.; Zhao, F. CO₂ Hydrogenation to Methanol on ZnO/ZrO₂ Catalysts: Effects of Zirconia Phase. *ChemistrySelect* **2021**, *6*, 2119–2125. [[CrossRef](#)]
12. Etim, U.; Song, Y.; Zhong, Z. Improving the Cu/ZnO-Based Catalysts for Carbon Dioxide Hydrogenation to Methanol, and the Use of Methanol as a Renewable Energy Storage Media. *Front. Energy Res.* **2020**, *8*. [[CrossRef](#)]
13. Etim, U.J.; Semiat, R.; Zhong, Z. CO₂ Valorization Reactions over Cu-Based Catalysts: Characterization and the Nature of Active Sites. *Am. J. Chem. Eng.* **2021**, *9*, 53–78. [[CrossRef](#)]
14. Dong, X.; Li, F.; Zhao, N.; Xiao, F.; Wang, J.; Tan, Y. CO₂ hydrogenation to methanol over Cu/ZnO/ZrO₂ catalysts prepared by precipitation-reduction method. *Appl. Catal. B Environ.* **2016**, *191*, 8–17. [[CrossRef](#)]
15. Natesakhawat, S.; Lekse, J.W.; Baltrus, J.P.; Ohodnicki, P.R., Jr.; Howard, B.H.; Deng, X.; Matranga, C. Active sites and structure–activity relationships of copper-based catalysts for carbon dioxide hydrogenation to methanol. *ACS Catal.* **2012**, *2*, 1667–1676. [[CrossRef](#)]
16. Huš, M.; Kopač, D.; Štefančič, N.S.; Jurković, D.L.; Dasireddy, V.D.; Likozar, B. Unravelling the mechanisms of CO₂ hydrogenation to methanol on Cu-based catalysts using first-principles multiscale modelling and experiments. *Catal. Sci. Technol.* **2017**, *7*, 5900–5913. [[CrossRef](#)]
17. Kuld, S.; Thorhauge, M.; Falsig, H.; Elkjær, C.F.; Helveg, S.; Chorkendorff, I.; Sehested, J. Quantifying the promotion of Cu catalysts by ZnO for methanol synthesis. *Science* **2016**, *352*, 969–974. [[CrossRef](#)]
18. Nitta, Y.; Suwata, O.; Ikeda, Y.; Okamoto, Y.; Imanaka, T. Copper-zirconia catalysts for methanol synthesis from carbon dioxide: Effect of ZnO addition to Cu-ZrO₂ catalysts. *Catal. Lett.* **1994**, *26*, 345–354. [[CrossRef](#)]
19. An, B.; Zhang, J.; Cheng, K.; Ji, P.; Wang, C.; Lin, W. Confinement of Ultrasmall Cu/ZnO_x Nanoparticles in Metal–Organic Frameworks for Selective Methanol Synthesis from Catalytic Hydrogenation of CO₂. *J. Am. Chem. Soc.* **2017**, *139*, 3834–3840. [[CrossRef](#)]
20. Dasireddy, V.D.; Likozar, B. The role of copper oxidation state in Cu/ZnO/Al₂O₃ catalysts in CO₂ hydrogenation and methanol productivity. *Renew. Energ.* **2019**, *140*, 452–460. [[CrossRef](#)]
21. Behrens, M.; Studt, F.; Kasatkin, I.; Kühl, S.; Hävecker, M.; Abild-Pedersen, F.; Zander, S.; Girgsdies, F.; Kurr, P.; Knief, B.-L. The active site of methanol synthesis over Cu/ZnO/Al₂O₃ industrial catalysts. *Science* **2012**, *336*, 893–897. [[CrossRef](#)]
22. Liang, B.; Ma, J.; Su, X.; Yang, C.; Duan, H.; Zhou, H.; Deng, S.; Li, L.; Huang, Y. Investigation on Deactivation of Cu/ZnO/Al₂O₃ Catalyst for CO₂ Hydrogenation to Methanol. *Ind. Eng. Chem. Res.* **2019**, *58*, 9030–9037. [[CrossRef](#)]
23. Narayanan, R.; El-Sayed, M.A. *Catalysis with Transition Metal Nanoparticles in Colloidal Solution: Nanoparticle Shape Dependence and Stability*; ACS Publications: Washington, DC, USA, 2005; pp. 12663–12676.
24. Sakpal, T.; Lefferts, L. Structure-dependent activity of CeO₂ supported Ru catalysts for CO₂ methanation. *J. Catal.* **2018**, *367*, 171–180. [[CrossRef](#)]
25. Lei, H.; Nie, R.; Wu, G.; Hou, Z. Hydrogenation of CO₂ to CH₃OH over Cu/ZnO catalysts with different ZnO morphology. *Fuel* **2015**, *154*, 161–166. [[CrossRef](#)]
26. Liao, F.; Huang, Y.; Ge, J.; Zheng, W.; Tedsree, K.; Collier, P.; Hong, X.; Tsang, S.C. Morphology—Dependent Interactions of ZnO with Cu Nanoparticles at the Materials’ Interface in Selective Hydrogenation of CO₂ to CH₃OH. *Angew. Chem. Int. Ed.* **2011**, *50*, 2162–2165. [[CrossRef](#)]
27. An, X.; Li, J.; Zuo, Y.; Zhang, Q.; Wang, D.; Wang, J. A Cu/Zn/Al/Zr fibrous catalyst that is an improved CO₂ hydrogenation to methanol catalyst. *Catal. Lett.* **2007**, *118*, 264–269. [[CrossRef](#)]
28. Huttunen, P.K.; Labadini, D.; Hafiz, S.S.; Gokalp, S.; Wolff, E.P.; Martell, S.M.; Foster, M. DRIFTS investigation of methanol oxidation on CeO₂ nanoparticles. *Appl. Surf. Sci.* **2021**, *554*, 149518. [[CrossRef](#)]
29. Reddy, K.P.; Choi, H.; Kim, D.; Choi, M.; Ryoo, R.; Park, J.Y. The facet effect of ceria nanoparticles on platinum dispersion and catalytic activity of methanol partial oxidation. *Chem Commun* **2021**, *57*, 7382–7385. [[CrossRef](#)]
30. Chen, K.; Fang, H.; Wu, S.; Liu, X.; Zheng, J.; Zhou, S.; Duan, X.; Zhuang, Y.; Tsang, S.C.E.; Yuan, Y. CO₂ hydrogenation to methanol over Cu catalysts supported on La-modified SBA-15: The crucial role of Cu–LaOx interfaces. *Appl. Catal. B Environ.* **2019**, *251*, 119–129. [[CrossRef](#)]
31. Zhu, J.; Su, Y.; Chai, J.; Muravev, V.; Kosinov, N.; Hensen, E.J. Mechanism and nature of active sites for methanol synthesis from CO/CO₂ on Cu/CeO₂. *ACS Catal.* **2020**, *10*, 11532–11544. [[CrossRef](#)]
32. Shen, S.; Chen, Q.; Chow, P.; Tan, G.; Zeng, X.; Wang, Z.; Tan, R.B. Steam-assisted solid wet-gel synthesis of high-quality nanorods of boehmite and alumina. *J. Phy. Chem. C* **2007**, *111*, 700–707. [[CrossRef](#)]
33. Bai, P.; Su, F.; Wu, P.; Wang, L.; Lee, F.Y.; Lv, L.; Yan, Z.-f.; Zhao, X.S. Copolymer-Controlled Homogeneous Precipitation for the Synthesis of Porous Microfibers of Alumina. *Langmuir* **2007**, *23*, 4599–4605. [[CrossRef](#)]
34. Martínez, A.; Prieto, G.; Rollán, J. Nanofibrous γ-Al₂O₃ as support for Co-based Fischer–Tropsch catalysts: Pondering the relevance of diffusional and dispersion effects on catalytic performance. *J. Catal.* **2009**, *263*, 292–305. [[CrossRef](#)]

35. Thommes, M.; Kaneko, K.; Neimark, A.V.; Olivier, J.P.; Rodriguez-Reinoso, F.; Rouquerol, J.; Sing, K.S. Physisorption of gases, with special reference to the evaluation of surface area and pore size distribution (IUPAC Technical Report). *Pure Appl. Chem.* **2015**, *87*, 1051–1069. [[CrossRef](#)]
36. Zhang, C.; Wang, L.; Etim, U.J.; Song, Y.; Gazit, O.M.; Zhong, Z. Oxygen vacancies in Cu/TiO₂ boost strong metal-support interaction and CO₂ hydrogenation to methanol. *J. Catal.* **2022**, *413*, 284–296. [[CrossRef](#)]
37. Wang, L.-X.; Guan, E.; Wang, Z.; Wang, L.; Gong, Z.; Cui, Y.; Yang, Z.; Wang, C.; Zhang, J.; Meng, X. Dispersed nickel boosts catalysis by copper in CO₂ hydrogenation. *ACS Catal.* **2020**, *10*, 9261–9270. [[CrossRef](#)]
38. Kattel, S.; Yan, B.; Yang, Y.; Chen, J.G.; Liu, P. Optimizing binding energies of key intermediates for CO₂ hydrogenation to methanol over oxide-supported copper. *J. Am. Chem. Soc.* **2016**, *138*, 12440–12450. [[CrossRef](#)]
39. Bansode, A.; Tidona, B.; von Rohr, P.R.; Urakawa, A. Impact of K and Ba promoters on CO₂ hydrogenation over Cu/Al₂O₃ catalysts at high pressure. *Catal. Sci. Technol.* **2013**, *3*, 767–778. [[CrossRef](#)]
40. Hu, J.; Li, Y.; Zhen, Y.; Chen, M.; Wan, H. In situ FTIR and ex situ XPS/HS-LEIS study of supported Cu/Al₂O₃ and Cu/ZnO catalysts for CO₂ hydrogenation. *Chin. J. Catal.* **2021**, *42*, 367–375. [[CrossRef](#)]
41. Bando, K.K.; Sayama, K.; Kusama, H.; Okabe, K.; Arakawa, H. In-situ FT-IR study on CO₂ hydrogenation over Cu catalysts supported on SiO₂, Al₂O₃, and TiO₂. *Appl. Catal. A Gen.* **1997**, *165*, 391–409. [[CrossRef](#)]
42. Baltrusaitis, J.; Jensen, J.H.; Grassian, V.H. FTIR spectroscopy combined with isotope labeling and quantum chemical calculations to investigate adsorbed bicarbonate formation following reaction of carbon dioxide with surface hydroxyl groups on Fe₂O₃ and Al₂O₃. *J. Phys. Chem. B* **2006**, *110*, 12005–12016. [[CrossRef](#)] [[PubMed](#)]
43. Sakong, S.; Groß, A. Dissociative adsorption of hydrogen on strained Cu surfaces. *Surf. Sci.* **2003**, *525*, 107–118. [[CrossRef](#)]
44. Fujita, S.-I.; Usui, M.; Ohara, E.; Takezawa, N. Methanol synthesis from carbon dioxide at atmospheric pressure over Cu/ZnO catalyst. Role of methoxide species formed on ZnO support. *Catal. Lett.* **1992**, *13*, 349–358. [[CrossRef](#)]
45. Bailey, S.; Froment, G.; Snoeck, J.-W.; Waugh, K. A DRIFTS study of the morphology and surface adsorbate composition of an operating methanol synthesis catalyst. *Catal. Lett.* **1994**, *30*, 99–111. [[CrossRef](#)]
46. Kim, Y.; Trung, T.S.B.; Yang, S.; Kim, S.; Lee, H. Mechanism of the surface hydrogen induced conversion of CO₂ to methanol at Cu (111) step sites. *ACS Catal.* **2016**, *6*, 1037–1044. [[CrossRef](#)]
47. Liu, C.; Liu, P. Mechanistic study of methanol synthesis from CO₂ and H₂ on a modified model Mo₆S₈ cluster. *ACS Catal.* **2015**, *5*, 1004–1012. [[CrossRef](#)]